Metal Bioaccumulation in Biofilms and Diatom Teratologies Reflect Legacy Mining in an Urban Stream: the case of Lone Elm Creek (Missouri, USA)

Laura Malbezin[1], Maya Bedoiseau[1], Jessica Wilson[2], Alba Argerich[2], Claude Fortin[1], Isabelle Lavoie[1].

[1] Institut national de la recherche scientifique, 490 rue de la Couronne G1K 9A9, Quebec City, QC, Canada

[2] College of Agriculture, Food & Natural Resources, University of Missouri, 303K Anheuser-Busch Natural Resources Building, Missouri, United States of America

Corresponding author: lmalbezin@outlook.fr

ORCID ID:

0000-0002-4544-7952 (Laura Malbezin)

0000-0002-2918-6297 (Isabelle Lavoie)

Abstract :

Biofilms are increasingly used as tools for biomonitoring disturbed environments, for example, in urban, agricultural, and mining contexts. In this study, we used biofilms as integrators and bioindicators of metal contamination of Lone Elm Creek, a highly contaminated stream within the Tri-State Mining District in Joplin, Missouri (USA). We sampled biofilms upstream and downstream of a mine adit and analyzed metal content (Fe, Zn, Cd and Pb), diatom assemblage composition, and the presence and severity of frustule teratologies. Physico-chemical analyses showed marked differences in nitrogen and oxygen concentrations at the first site downstream of the mine adit. Metal concentrations in the water were elevated at all sites and did not vary markedly along the upstream-downstream gradient. In addition to metallic contamination from mine tailings, legacy of past activities may represent other sources of contamination. Diatom assemblage composition differed markedly at the site immediately downstream of the mine adit compared to other sites. The presence of frustule deformities as well as their type and their severity were investigated. *Ulnaria ulna*, *Achnantidium*

minutissimum, and *Fragilaria austriaca* were the most frequently deformed diatoms and showed the most severe abnormalities. However, the percentage of teratologies was not correlated with metal concentrations in the water or in the biofilm. Metal bioaccumulation in the biofilm as a function of metal concentration in the water fitted well to predictive models developed in previous studies, highlighting the potential of biofilms to be used as a tool to assess exposure to metal contamination.

Keywords:

Diatoms, Biofilm, Mining site, Metal bioaccumulation, Deformities

Declarations:

Funding –

JW was funded by the MU Center for Agroforestry. AA was funded by USDA NIFA McIntire-Stennis No.1016163. Funding by the Natural Sciences and Engineering Research Council of Canada, Discovery grant (RGPIN-2019-06823) to Claude Fortin, is acknowledged.

Competing interests –

The authors declare that they have no conflict of interest or competing interests.

Availability of data and material –

All data are available in supplementary information.

Code availability –

Not applicable.

Authors' contributions –

All authors made substantial contributions to this paper. L.M was in charge of data acquisition, data analysis, writing. M.B was in charge of data acquisition, data analysis, reviewing and editing. J.W was in charge of experimental conceptualization, sample collection, reviewing and editing. A.A was in charge of funding acquisition, project conception, reviewing and editing. C.F was in charge of data analysis, reviewing and editing. I.L was in charge of data analysis, reviewing and editing.

Acknowledgments –

Authors would like to thank Kim Racine of *Institut national de la recherche scientifique* for her help on metal analysis in ICP-OES and ICP-MS.

1. Introduction

Growing population and development of new technologies have led to an increasing demand for several natural resources, including metals. However, the extraction and use of these mineral resources can result in elevated environmental metal concentrations with significantly higher levels than their geochemical background. For example, phosphate fertilizers used in agriculture may be a source of nickel, cadmium, and lead in soils (Nziguheba and Smolders, 2008). These elements may be discharged directly into water bodies or transported from soils to aquatic ecosystems by leaching, subsequently jeopardizing freshwater organisms. The extent of the impact of these metals once in aquatic environments will depend on their speciation, i.e., changes in chemical forms as a function of environmental conditions where the free metal ion concentration is the main driver of bioavailability. Metal speciation conditions their affinity with biological ligands at the solution-organism interface, which can be predicted based on the biotic ligand model (BLM) (Campbell *et al*., 2002; Zhao *et al*., 2016). Once internalized, metals can affect cell integrity and impair organisms, with effects that can cascade along the trophic chain (Ali and Khan, 2019; Zhang *et al*., 2016).

Environmental monitoring programs, including assessments of metal contamination, are often based solely on the physico-chemical characteristics of the water. However, spot measurements do not always reflect effective exposure conditions, i.e., they do not integrate the bioavailability of chemicals as a function of temporal fluctuations in environmental conditions or the additive/synergistic/antagonistic effects in which the biological compartment evolves. In contrast, biota constantly interacts with its environment and thus integrates the physical, chemical, and biological changes in its surrounding environment. This is why biological components such as fish (Plessl *et al*., 2017), invertebrates (Bonada *et al*., 2006; Buss *et al*., 2015), diatoms (Charles *et al*., 2019; Lavoie *et al*., 2014; Rimet, 2012), and periphytic biofilms are widely used as biological indicators of ecosystem health (Griffith *et al*., 2005; Leguay *et al*., 2016).

Periphytic biofilms are a consortium of bacteria, archaea, algae, fungi, and protozoa embedded in an exopolysaccharide matrix (Guasch *et al*., 2016; Wetzel, 1983). They grow on any kind of substrate and are particularly abundant on rocky substrates along riverbeds or shallow lake sections. Periphytic biofilms represent a biological compartment of interest in aquatic ecosystem monitoring because they are ubiquitous and respond rapidly to environmental fluctuations (Battin *et al*., 2016; Sabater *et al*., 2007). At the basis of the food

web, periphytic biofilms are also a key component of aquatic and terrestrial environments. This "model organism" has been used to assess the effects of various disturbances (e.g., inorganic and organic contaminants (Cattaneo *et al*., 2004; Rimet and Bouchez, 2011), excess nutrients (Lei *et al*., 2021), and climate change (Virta and Teittinen, 2022)) based on a wide diversity of biological endpoints (e.g., photosynthesis, chlorophyll a, assemblage structure, oxidative stress, lipid composition). They have also been used as integrators of metal contamination, i.e., as proxies of bioavailable metals in the water. Indeed, periphytic biofilms are remarkable indicators of metal exposure; strong correlations have been observed between free metal concentrations in the water and bioaccumulated metals in the biofilm (Bradac *et al*., 2010; Laderriere *et al*., 2022, 2021; Leguay *et al*., 2016; Tien and Chen, 2013). The relationship between free metals and biofilm bioaccumulated metals may allow for a better estimate of metal exposure by integrating fluctuations in free metal concentrations over a longer time scale, thus providing a more appropriate assessment of metal exposure for the biota than spot measurements of metals in water. From a practical point of view, the metal accumulation observed within the biofilm also allows for the use of less sensitive and, therefore, less expensive analytical techniques, such as Inductively Coupled Plasma - Optical Emission Spectroscopy (ICP-OES) instead of Inductively Coupled Plasma - Mass Spectrometry (ICP-MS) typically required to measure low dissolved metal concentrations. Once accumulated in the biofilm, metals may potentially be transferred to consumers, and thus, may represent a source of exposure for these organisms (Fadhlaoui *et al.*, 2024; Wen *et al*., 2024; Xie *et al*., 2010). Biofilm metal content may therefore be a relevant metric for the risk assessment of metal contamination in aquatic ecosystems.

Diatoms are often the predominant group within periphytic biofilms (Blinn *et al*., 1980). These microalgae are widely used in stream biomonitoring (Lavoie *et al*., 2010; Lobo *et al*., 2016; Prygiel *et al*., 2002) as well as in paleolimnological studies (Balasubramaniam *et al*., 2023; Pillsbury *et al*., 2021) as they exhibit rapid changes in assemblage structure in response to environmental fluctuations. In addition to presenting specific environmental preferences and tolerances, making them excellent bioindicators, diatoms also exhibit morphological aberrations under certain environmental stresses, such as metal contamination. Indeed, teratologies observed on the siliceous shell of the diatoms (frustules) represent valuable biomarkers of metal exposure (Falasco *et al*., 2021; Lavoie *et al*., 2018; Smucker and Vis, 2009).

In this study, we used periphytic biofilm to assess metal contamination along a small urban watercourse with a legacy of metal mining (Lone Elm Creek, Joplin, Missouri, USA).

More specifically, our objectives were (1) to investigate the relationship between free metal concentrations in surface water and bioaccumulated concentrations of metals in periphytic biofilm, (2) to determine if metal bioaccumulation in the biofilm from Lone Elm Creek fits the values from published models, and (3) to assess diatom assemblage composition and the occurrence of teratologies.

2. Materials and methods

2.1. Study site

Lone Elm Creek (LEC) is a first-order urban stream in Joplin (Missouri, USA) located within the Tri-State Mining District (37.0922°N, 94.5274°W). The Tri-State Mining District (TSMD) was a global producer of lead (Pb) and zinc (Zn) from the 1850s to the 1960s with Joplin, Missouri, serving as an epicenter of metal production (McCauley *et al*., 1983). Joplin is now part of the Oronogo-Duenweg Superfund Site commonly known for extensive metal contamination from legacy smelter dust, waste ore piles, and point source discharges from abandoned mine shafts (i.e., mine adits) (USEPA, 2020). The chat piles when initially abandoned were recorded to extend for hundreds of meters above the ground before removal and remediation decades later (Gutierrez *et al*., 2019; Johnson *et al*., 2016). It is well documented that the chat piles not only contained elevated concentrations of Pb and Zn but other metals such as cadmium (Cd), silver (Ag), copper (Cu), and thallium (TI) that readily leached into surrounding soils, surface water, and groundwater (Beyer *et al*., 2004; Gibson, 1972; Gutierrez *et al*., 2019, 2015; Stefanowicz *et al*., 2014).

Joplin, Missouri, lies within the Springfield Plateau and Ozark Highlands ecoregion. The Springfield Plateau is part of the Mississippi Boone Formation and contains parent material from carbonate rocks and shale (Thompson, 1995). The area has karst topography marked by sinkholes, caves, and losing streams and dominated by soluble rocks such as limestone and dolomite. Ore within the TSMD is of the Mississippi Valley-Type (MVT) formation consisting mostly of sulfide forms of galena (PbS) and sphalerite (ZnS) along with small amounts of chalcopyrite ($CuFeS^2$) (Gutierrez et al., 2019). There are high concentrations of Cd found in ZnS within the MVT formation due to the direct substitutions with Zn (Zn^{2+} <-> Cd^{2+}), where Cd can replace Zn up to 5 percent (Gutierrez *et al*., 2019; Wen *et al*., 2016).

Joplin, Missouri, has a continental climate, denoted by large fluctuations in air temperature. In 2019, we observed an average air temperature during summer months of 24.7±2.4°C (average±standard deviation), and of 5.0±6.2°C during winter months. Joplin receives an average of 118 cm of precipitation a year (National oceanic and atmospheric administration, 2020). In 2019, the region received a total of 59.9 cm during summer months and 22.6 cm during winter months. Average air temperature during our November sampling for periphytic biofilms was 6.74°C, and total precipitation reached a total of 6.45 cm.

Lone Elm Creek is mostly contaminated with lead, cadmium, zinc, and iron (Fe) most likely from both legacy smelter dust and the discharge from a mine adit of the historic underground Black Diamond mine that flows for 100 meters along a residential road before discharging into the downstream reach (Wilson, 2023). The LEC study site was split into a 100-m upstream reach (US), and a 230-m downstream reach (DS) based on the location of the mine adit (Figure 1). Seven sampling sites were designated in the US (US1 – US7), and seven in the DS (DS1 – DS7). The US and DS have concrete lined bed and banks with mixed substrate consisting of silt-sand, gravel, cobble, and boulders. Both the US and DS have open canopies with year-round sunlight and receive run-off from impervious surfaces (i.e., parking lots and roads), and from commercial and residential lawns. Discharge during the November sampling was 17±5 $L \cdot s^{-1}$ at the US, and 22±5 $L \cdot s^{-1}$ at the DS.

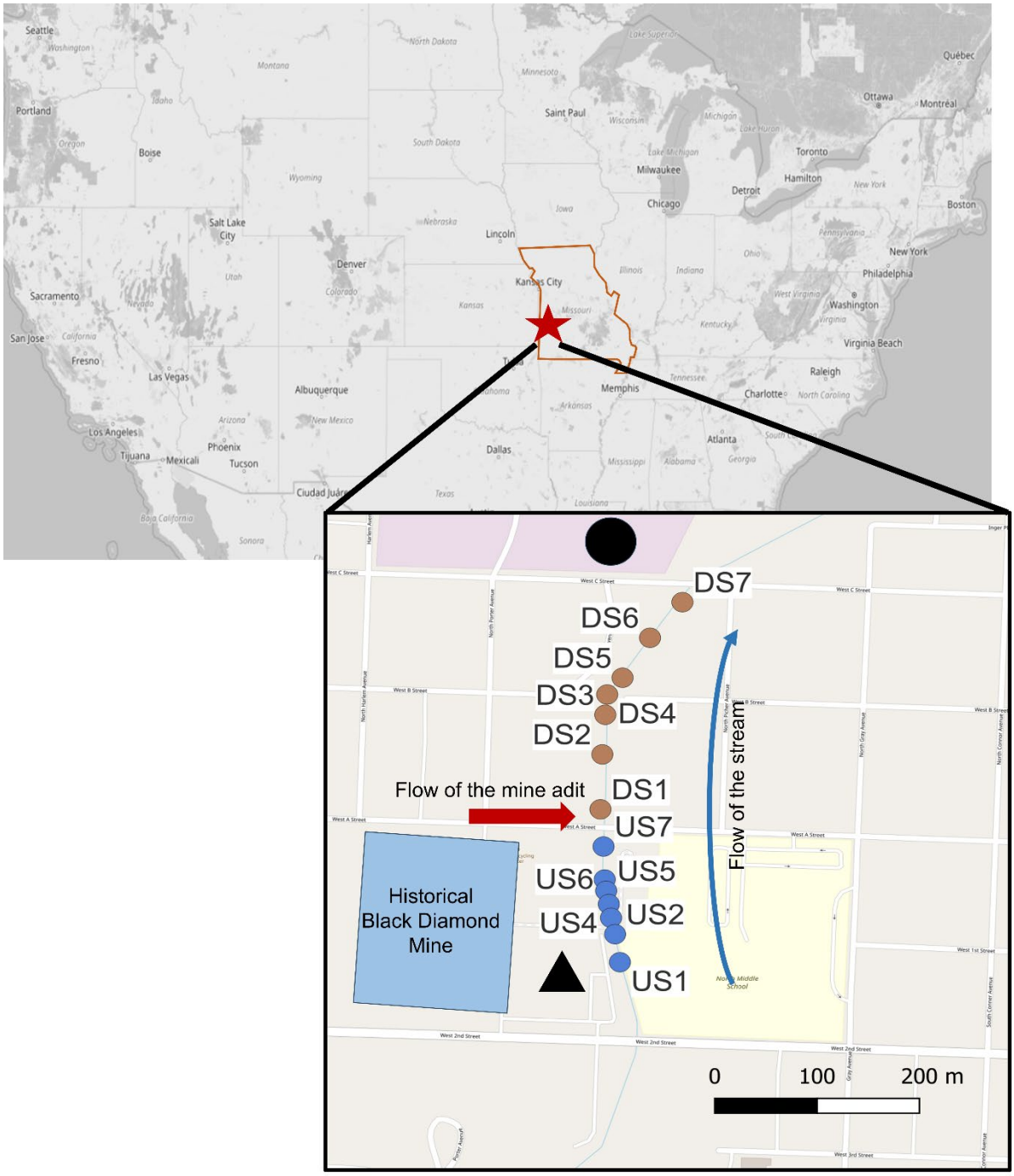

Figure 1: Map of the study sites. Lone Elm Creek in Joplin (Missouri, USA) is surrounded by legacy mining operations such as the historical Black Diamond Mine, a recycling center (black triangle), industrial warehouses (black circle), residential housing and a school (made with QGIS 3.36.3).

2.2. Surface water analyses and metal speciation calculations

We sampled water for chemical analyses in November 2019. On each of the sampling sites, we measured water temperature, specific conductivity (SpC), dissolved oxygen saturation (%DO), and pH with an EXO1 multiparameter probe (YSI©, xylem brand). Simultaneous surface water samples were also taken for ammonium (NH_4^+-N), nitrate, and nitrite (NO_3^- -N + NO_2^- -N), soluble reactive phosphorus (SRP), and dissolved organic carbon (DOC) analyses. Water samples were collected in triplicate at each of the sampling sites with 60 mL syringes that had been pre-rinsed with the corresponding surface water, filtered upon collection with 0.7 µm pre-ashed GF/F filters, immediately placed on ice, and frozen until laboratory analysis. NH_4^+-N and NO_3-N + NO_2^- -N were analysed by Flow Injection Analysis (FIA) with a Lachat QuickChem 8500 Series 2 using automated phenate, and automated cadmium reduction methods with detection limits of 0.01 mg $N \cdot L^{-1}$ and 0.005 mg $N \cdot L^{-1}$, respectively (APHA-4500-NH3G; APHA-4500-NO3F). SRP was analyzed by a Genesys 2 Spectrophotometer using ascorbic acid without persulfate digestion with a detection limit of 0.001 mg $P \cdot L^{-1}$ (APHA-4500-P.E), while DOC was analyzed as Nonpurgeable Organic Carbon (NPOC) with a Shimadzu TOC-V CPH by oxidative combustion and infrared analysis with detection limit of 0.1 mg $C \cdot L^{-1}$ (APHA-5310B).

For metal analysis, water samples were collected at each site using clean 30 mL polypropylene syringes (Thermo Scientific™ National Target All-Plastic Disposable Syringes with polypropylene barrels and polyethylene plungers), immediately filtered with 0.45 µm pore size membrane filters (Whatman 7184-004 Cellulose Nitrate Membrane Filter, 47 mm Diameter), and then acidified with nitric acid (HNO_3) within 48 h, and stored at 4 °C until analysis within 2 weeks. Dissolved metal concentrations were analyzed by ICP-MS (limit of detection (LOD): 2.0 $\mu g \cdot L^{-1}$ for iron, 0.1 $\mu g \cdot L^{-1}$ for zinc and 0.01 $\mu g \cdot L^{-1}$ for cadmium and lead) by the Columbia Environmental Research Center (CERC), a local branch of the U.S. Geological Survey (USGS). Results below the detection limit were replaced by the LOD/2 value when required. Metal concentrations were measured for water samples collected in July, August, and November 2019. The August and November 2019 water samples could not be filtered within 1-2 h after collection unlike the July 2019 samples. This may have resulted in greater iron precipitation in samples from these dates, and thus to underestimate iron concentrations in the water. Metal concentrations (other than iron) did not show any significant

differences between the different dates. Therefore, we selected metal concentration data from July 2019 for our analyses of biofilm metal contents.

The software Windermere Humic Aqueous Model VII (WHAM) was used to estimate metal speciation in the water collected at each site (Tipping *et al*., 2011) using pH, DOC and a reference value of 200 $mg \cdot L^{-1}$ for water hardness (U.S. Geological Survey, 2019) as input parameters. To facilitate comparison with previous studies, free ion concentrations have been presented; however, the rest of metal species have not been included. Cumulative criterion unit (CCU) was used as proxy of metal toxicity (Lavoie *et al*., 2018; Morin *et al*., 2012) and is defined as the ratio of measured metal concentrations in the water over the United States Environmental Protection Agency (U.S.EPA) criterion continuous concentration (CCC) (USEPA, 2023). The CCU is given as:

$$CCU = \sum_{i=1}^{n} mi/ci$$

where *mi* is the total recoverable metal concentration and *ci* is the criterion continuous concentration (CCC; chronic) for each metal (Clements *et al*., 2000). The criterion continuous concentration for iron was 1000 $\mu g \cdot L^{-1}$. As water hardness strongly influences Cd, Pb, and Zn bioavailability, we used the reference values for hardness (200 $mg \cdot L^{-1}$) to account for this parameter in determining a modified criterion (USEPA, 2023). We obtained 1.2 $\mu g \cdot L^{-1}$ for Cd, 5.3 $\mu g \cdot L^{-1}$ for Pb, and 212.5 $\mu g \cdot L^{-1}$ for Zn.

2.3. Biofilm sampling

Biofilm was not collected from US1 and US2 because of the lack of hard benthic substrate while US3 was not sampled because of the presence of an inaccessible pool. Thus, biofilm was collected from US4 to US7 and from DS1 to DS7 during November 2019 (Figure 2). The periphyton was sampled by scraping the surface of five removable rocks from the streambed with a scoopula. Then, the sample was homogenized and redistributed to form four composite samples. Samples were stored into pre-rinsed 50 mL VWR® sterile, metal-free, polypropylene centrifuge tubes and immediately placed on ice. Upon return to the University of Missouri laboratory, samples were kept overnight at 4°C, centrifuged to remove excess water and frozen at -18°C until samples were freeze-dried. Freeze-dried periphyton samples (1-5 g of dry weight) were shipped to the laboratory of the Institut national de la recherche scientifique, Centre Eau Terre Environnement (INRS-ETE) in Quebec City, Canada, for further metal bioaccumulation analyses and microscopic observations (see sections 2.4 – 2.5 for details).

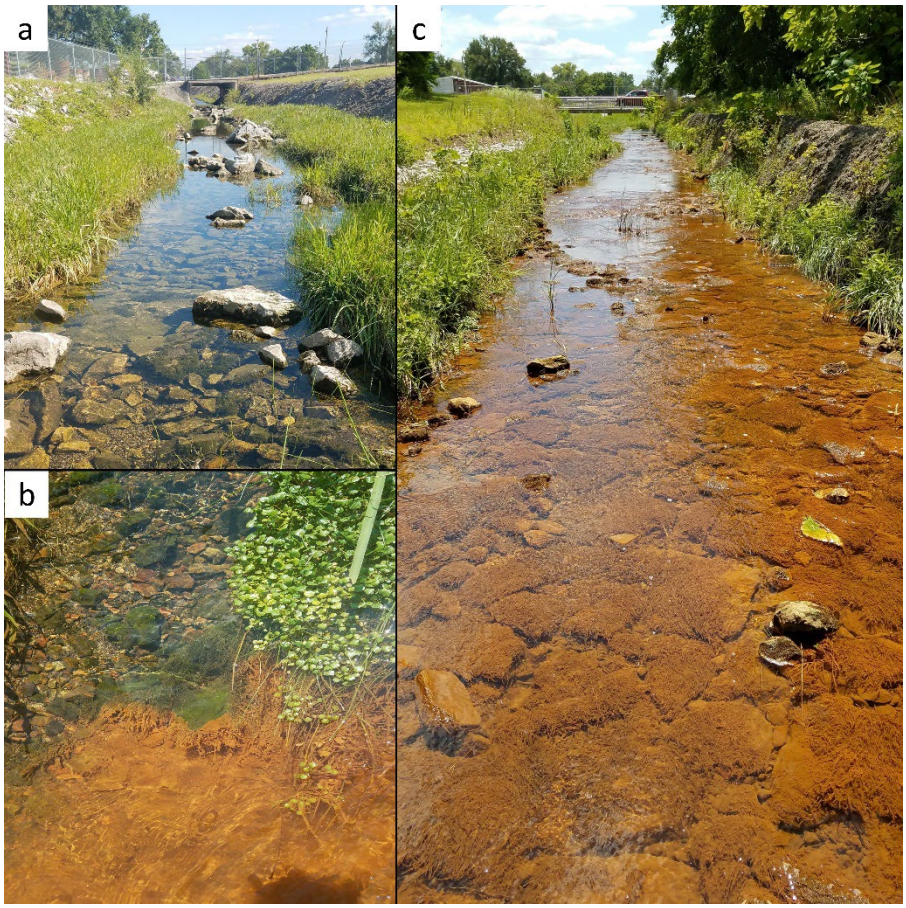

Figure 2: Study reaches and mine adit at Lone Elm Creek. (A) Upstream reach (US), (B) input from the mine adit, and (C) downstream reach (DS).

2.4. Metal bioaccumulation in biofilm and diatom frustule observations

For all samples, 50 mg of freeze-dried biofilm was digested in a 50 mL tube (Polypropylene, Sarstedt) by adding 800 µL of concentrated HNO_3 (TraceMetal™ grade, Fisher). After 48 h, 200 µL of 30% H_2O_2 (Optima™ grade, Fisher) was added for another 48 h. An aliquot of 400 µL of supernatant was transferred to a 13 mL tube (Polypropylene, Sarstedt) with 3.6 mL of ultra-pure water (Milli-Q) for a final volume of 4 mL and stored at room temperature until analysis. The remaining pellets of digested periphytic biofilm were kept for the observation of diatom frustules. Pellets were rinsed with tap water, adjusting the volume of water to 50 mL, and then centrifuged for 10 min at 5500 rpm. The supernatant was discarded, and these steps were repeated until the pH reached ≥ 6.

To quantify the metals accumulated in the biofilm, the samples were diluted by a factor of 150 with 10% HNO_3 prepared from concentrated TraceMetal™ grade HNO_3 and ultra-pure water prior to analysis. Fe and Zn were analyzed by ICP-OES (Varian Inc. 725-ES ICP-OES; Zn_{LOD}=0.005 µg·L^{-1}, Fe_{LOD}=0.020 µg·L^{-1}), while Cd and Pb, present at lower concentrations, were analyzed by ICP-MS (Thermoscientific XSeries 2; Cd_{LOD}=0.009 µg·L^{-1}, Pb_{LOD}=0.01 µg·L^{-1}). Measurements of metals accumulated in the biofilm were independently conducted for each composite sample (n=4 per site).

For each metal and all samples, the log of bioconcentration factor (BCF) was calculated as the log of the ratio of the concentration of the metal in the biofilm sample and the total concentration of the same metal in the stream water. The BCF is given as:

$$BCF = \frac{C}{Cw}$$

where C is the metal concentration in biofilm (mol·Kg^{-1}) and Cw is the metal concentration in water (mol·L^{-1}).

2.5. Diatom slide preparation and microscopic observations

Digested diatom frustules were mounted onto microscope slides using Naphrax® (Brunel Microscopes, UK) as a mounting medium. For each site, four slides were prepared for diatom assessment. Diatom assemblage composition and deformities were investigated using

an optical upright microscope (Carl Zeiss Ltd Axio Imager 2) with immersion oil at x1000 magnification. On each slide, at least 500 diatom valves were identified. The analysis also consisted in determining the severity (low, medium, high) and the type (raphe, striae, overall shape) of deformations observed. The data from the four replicates were averaged and counts were expressed as relative abundances (%). Taxonomic identifications followed Lavoie *et al*., (2008) and Bey and Ector, (2013).

2.6. Statistical analyses

All statistical analyses were performed with RStudio (R version 4.3.2). Residuals plots were generated to assess normality and homogeneity of variance. To investigate the differences in physico-chemical parameters between US and DS reaches, as well as to compare metal concentrations in the water and metal concentration in the biofilm between both reaches, we used Student's test or Wilcoxon rank sum test, depending on whether the requisite assumptions were met. Linear regressions of biofilm metal content as a function of calculated free metal concentration in water were performed on SigmaPlot (version 13, Systat Software, Inc., San Jose, California, USA) using data from Laderriere *et al*., (2021), (2020) and Leguay *et al*., (2016). We added data from the current study to examine the fit with existing models. A Student's test was used to compare average frustule deformities at each sampling site to the threshold of 0.5%, which represents an estimate of the natural occurrence of deformed diatoms (Morin *et al*., 2008a). The same test was used to compare the occurrence of deformities in US and DS reaches.

3. Results

3.1. Water physico-chemistry

Water chemistry data were previously presented in Wilson, (2023) for the period from September 2019 to February 2020. On the biofilm sampling date (November 2019), the water temperature was similar in US and DS, at approximately 12°C, except for the DS1 site (17.1°C). The pH was similar among US and DS sites (Table 1), with a mean of and 7.60±0.02 in US and 7.56±0.18 in DS, indicating a circumneutral pH. Specific conductivity in the DS

reach (1134±145 µS·cm^{-1}) was significantly higher than in the US reach (979±4 µS·cm^{-1}; Wilcoxon test, df=9, W=28, p-value<0.05). In general, US presented higher average %DO than DS (128.6±1.5% and 107.7±16.6%, respectively; Wilcoxon test, df=9, W=0, p-value<0.05). The site DS1 exhibited the lowest %DO (70%) as well as the highest ammonium (NH_4^+) concentrations and lower nitrate concentrations. Between DS1 and DS2 sites, water physico-chemistry returned to values comparable to those observed in the US portion of the study area, with a water temperature decreasing by 3.9°C and a decrease in specific conductivity of 378 µS·cm^{-1}, while the %DO increased from 70.2% to 111.4%. Values continued to change from DS2 to DS7, but not as drastically. Indeed, we only observed a 1.0°C decrease in water temperature, a 10 µS·cm^{-1} decrease in specific conductivity, and a 5.6% increase in percent oxygen saturation. In contrast to the DS reach of the study area, temperature, oxygen, and conductivity exhibited low variability among the US4 to US7 sites.

Table 1: Water chemistry monitored in all sampling sites on November 2019 sampling date.

Reach	**Sampling Site**	**T (°C)**	**Specific conductivity (µS·cm^{-1})**	**pH**	**%DO**	**NH_4^+-N (mg·L^{-1})**	**NO_3^--N (mg·L^{-1})**	**SRP (mg·L^{-1})**	**DOC (mg·L^{-1})**
Upstream	4	12.0	974.0	7.63	128.9	<0.01	0.872	0.002	1.9
Upstream	5	12.1	981.0	7.58	127	<0.01	0.958	0.002	1.9
Upstream	6	12.1	982.0	7.59	129.9	<0.01	0.926	0.002	1.9
Upstream	7	12.1	978.0	7.60	130.1	<0.01	0.920	0.003	1.9
Downstream	1	17.1	1461.0	7.20	70.2	0.33	0.012	0.002	1.7
Downstream	2	13.2	1083.0	7.49	111.4	0.09	0.930	0.001	1.9
Downstream	3	13.2	1088.0	7.53	112.7	0.07	0.969	0.003	1.8
Downstream	4	12.9	1083.0	7.60	113.1	0.05	1.033	0.002	1.7
Downstream	5	12.7	1072.0	7.65	114	0.05	1.117	0.002	1.7
Downstream	6	12.5	1075.0	7.72	115.2	0.04	1.053	0.002	1.7
Downstream	7	12.2	1073.0	7.73	117	0.03	1.060	0.002	1.8

NH_4^+-N in the US reach was below the detection limit while the DS reach showed average concentrations of 0.09±0.11 mg N·L^{-1}. Nitrate (NO_3^--N) and dissolved organic carbon (DOC) concentrations were slightly higher in the US sampling sites (respectively, 0.92±0.04 mg N·L^{-1} and 1.93±0.05 mg C·L^{-1}) than in the DS sites (respectively, 0.88±0.39 mg N·L^{-1} and

1.54±0.16 mg $C \cdot L^{-1}$), while SRP was similar between the US and DS reaches (0.002±0.001 mg $P \cdot L^{-1}$). Dissolved nutrient concentrations showed low variability between US4 to US7 sites, while NH_4^+-N, NO_3^--N, and DOC concentrations drastically changed at DS1. Indeed, DOC decreased, while NH_4^+-N and NO_3^--N concentrations showed opposing trends where NH_4^+-N increased and NO_3^--N decreased. Values sharply returned close to average values at DS2, and slight decreasing and increasing trends from DS2 to DS7 in NH_4^+-N and NO_3^--N concentrations, respectively, were observed. DOC concentrations were not spatially different from DS2 to DS7 (Table 1).

Table 2: Total metal concentrations ($mol \cdot L^{-1}$) and cumulative criterion unit (CCU) in water from the upstream (US) and downstream (DS) sites along the Lone Elm Creek.

Sampling site	**Fe**	**Zn**	**Cd**	**Pb**	**CCU**
US4	$1.36x10^{-5}$	$5.97x10^{-5}$	$1.71x10^{-7}$	$1.83x10^{-9}$	35.1
US5	$1.40x10^{-5}$	$6.13x10^{-5}$	$1.69x10^{-7}$	$2.08x10^{-9}$	35.4
US6	$1.36x10^{-5}$	$5.46x10^{-5}$	$1.54x10^{-7}$	$2.36x10^{-9}$	32.0
US7	$1.40x10^{-5}$	$4.94x10^{-5}$	$1.43x10^{-7}$	$1.69x10^{-9}$	29.4
DS1	$3.94x10^{-5}$	$4.30x10^{-5}$	$5.68x10^{-8}$	$9.17x10^{-10}$	20.7
DS2	$2.33x10^{-5}$	$3.84x10^{-5}$	$5.03x10^{-8}$	$1.01x10^{-9}$	17.8
DS3	$1.79x10^{-5}$	$3.62x10^{-5}$	$4.64x10^{-8}$	$2.41x10^{-10}$	18.6
DS4	$1.79x10^{-5}$	$4.18x10^{-5}$	$5.01x10^{-8}$	$1.25x10^{-9}$	16.5
DS5*	$1.79x10^{-5}$	$3.67x10^{-5}$	$4.73x10^{-8}$	$9.65x10^{-10}$	15.7
DS6	$1.79x10^{-5}$	$3.17x10^{-5}$	$4.46x10^{-8}$	$6.76x10^{-10}$	14.9
DS7	$1.50x10^{-5}$	$1.99x10^{-5}$	$3.71x10^{-8}$	$5.31x10^{-10}$	10.4

* Metal concentrations at DS5 were estimated by averaging DS4 and DS6 values.

Dissolved metal concentrations in surface water along the LEC are reported in Table 2. To circumvent the absence of metal concentrations at site DS5 and considering the similarity in geomorphology between sites DS4 and DS5 and the similarity between the physico-chemical parameters at DS4 and DS6, metal concentrations at site DS5 were estimated based on the average of the metal concentrations obtained at sites DS4 and DS6. Zn was the metal showing the highest concentrations, followed by Fe, Cd, and Pb. Zn concentrations were slightly higher in US ($5.62x10^{-5}$±$5.39x10^{-6}$ $mol \cdot L^{-1}$) than in DS ($3.54x10^{-5}$±$7.79x10^{-6}$ $mol \cdot L^{-1}$) (Student's test, df=9, t=-4.7, p-value<0.01), decreasing along the river between US4 and DS3 sites, and slightly

increasing at DS4 and decreasing again at DS7. In general, Pb concentrations were higher in US than in DS (Student's test, df=9, t=-6.1, p-value<0.001), but peaked at DS1 and were the lowest at DS7. Cd concentrations were higher in US (Wilcoxon Mann-Whitney, df=9, W=0, p-value<0.01), decreased at DS1 and remained relatively constant in DS. Metal speciation calculations using the WHAM model indicated that both Cd and Zn were mostly present in the free-ion form (95 to 98% for Cd and 75 to 91% for Zn) while 7 to 30% of the dissolved Pb was free. Other species considered were hydroxo- and carbonato-complexes as well as binding to dissolved organic matter. For Cd, these species were all ≤ 2%. For Zn, organic complexes were between 3 and 5% while up to 6% were hydroxo-complexes and up to 14% carbonato-complexes. Finally, Pb was mostly bound to carbonates (27 to 67%), organic matter (21 to 35%) and hydroxides (6 to 8%). Full metal speciation distribution is available in Supplementary Information.

CCU values ranged between 35.4 (US5) and 10.4 (DS7) (Table 2). The highest CCU values were obtained for US sites with mean CCU of 33.0±2.9, while mean CCU was 16.4±3.3 for DS sites. Cd and Zn water concentrations greatly exceeded water quality criteria at all sites, while Fe exceeded criteria only at the DS1 and DS2. Pb concentrations remained below the criterium.

3.2. Metal concentrations in biofilms

Metal concentrations in the biofilm were much higher than in the water, suggesting a bioaccumulation of metals in the biofilm. Zn and Pb were slightly more bioaccumulated at the DS reach than US (Student's test, df=9, both p-value<0.05, t=2.6 for Zn and t=4.5 for Pb), while bioaccumulated Cd levels were stable along the gradient (Student's test, non-significant p-value) except for DS1 where it was especially low (Figure 3). In parallel, Fe was more abundant in biofilm in the sites located downstream of the discharge area than in the sites located upstream (Student's test, df=9, t=3.4, p-value<0.01), which is consistent with the Fe concentrations in surface water (average metal free form concentrations in water and metal concentrations in biofilm are available in Supplementary Information, Table 3). In general, metal concentrations in the water and in the biofilm followed a similar pattern where Zn and Fe were the most bioaccumulated metals followed by Cd and Pb.

For all studied metals, the log of bioconcentration factors or log(BCFs) was higher in the DS of the study area compared to the US (Values of log(BCF) are given in Supplementary Information, Table 4). The log(BCF) of Fe varied from 3.8±0.1 in the US to 4.9±0.1 in the DS, while Zn varied from 3.7±0.1 to 4.1±0.2, Cd varied from 4.0±0.1 to 4.2±0.6, and Pb from 5.4±0.1 to 6.0±0.2. Log(BCFs) for Fe, Cd, and Pb were the highest at DS3 (respectively 5.1, 4.4 and 6.3), while the highest Zn log(BCF) was observed at DS7 (4.3).

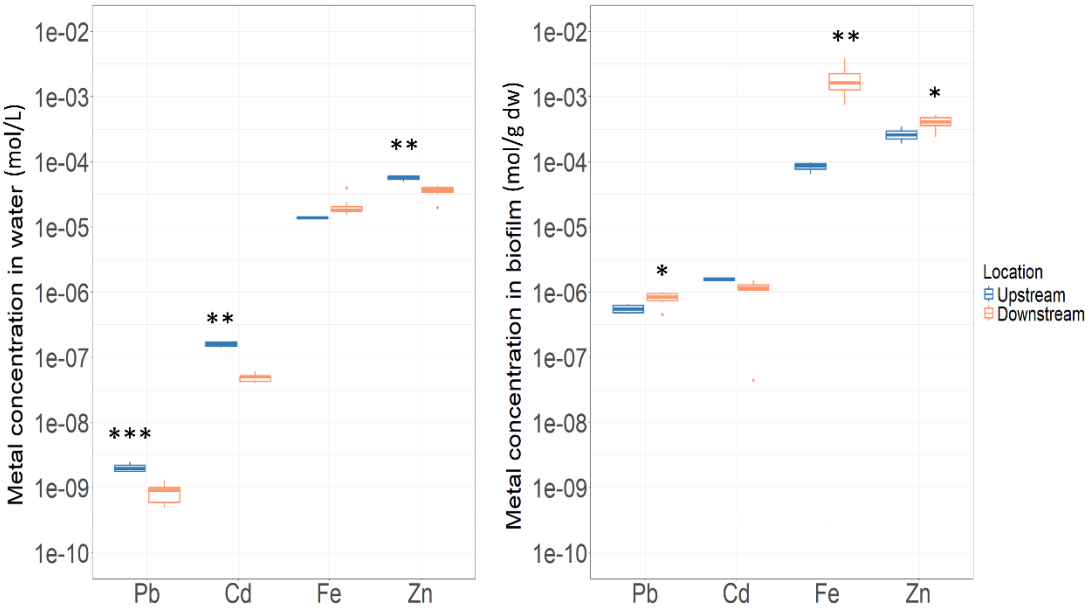

Figure 3: Total metal concentrations at upstream versus downstream reaches for water and biofilm (n=4) (* p-value<0.05, ** p-value<0.01 and *** p-value<0.001).

3.3. Fitting with bioaccumulation models

The range in predicted free metal concentrations in our water samples was relatively narrow in this study. To put these results in perspective, we compared our data with previously published ones (Leguay *et al.,* 2016; Laderriere *et al*., 2020, 2021). In these publications, the authors used datasets from various mining sites (abandoned, rehabilitated and operating sites) spanning a wide geographical range within the provinces of Quebec and Ontario (Canada) and found strong relationships between free metals in the water and bioaccumulated metals in the biofilm at circumneutral pHs (>6). We added our data to these regression models to determine if the data from Lone Elm Creek fit previously observed distributions. We ran new regression analyses including previously published data (black) as well as the data from the present study (red) and found that the majority of our observations for cadmium and zinc were distributed at the high end of the concentration range, while those for lead were distributed in the middle of the range (Figure 4). For all three metals, values obtained in this study agreed with previous models (with comparable pHs between studies (6 and 7.7)).

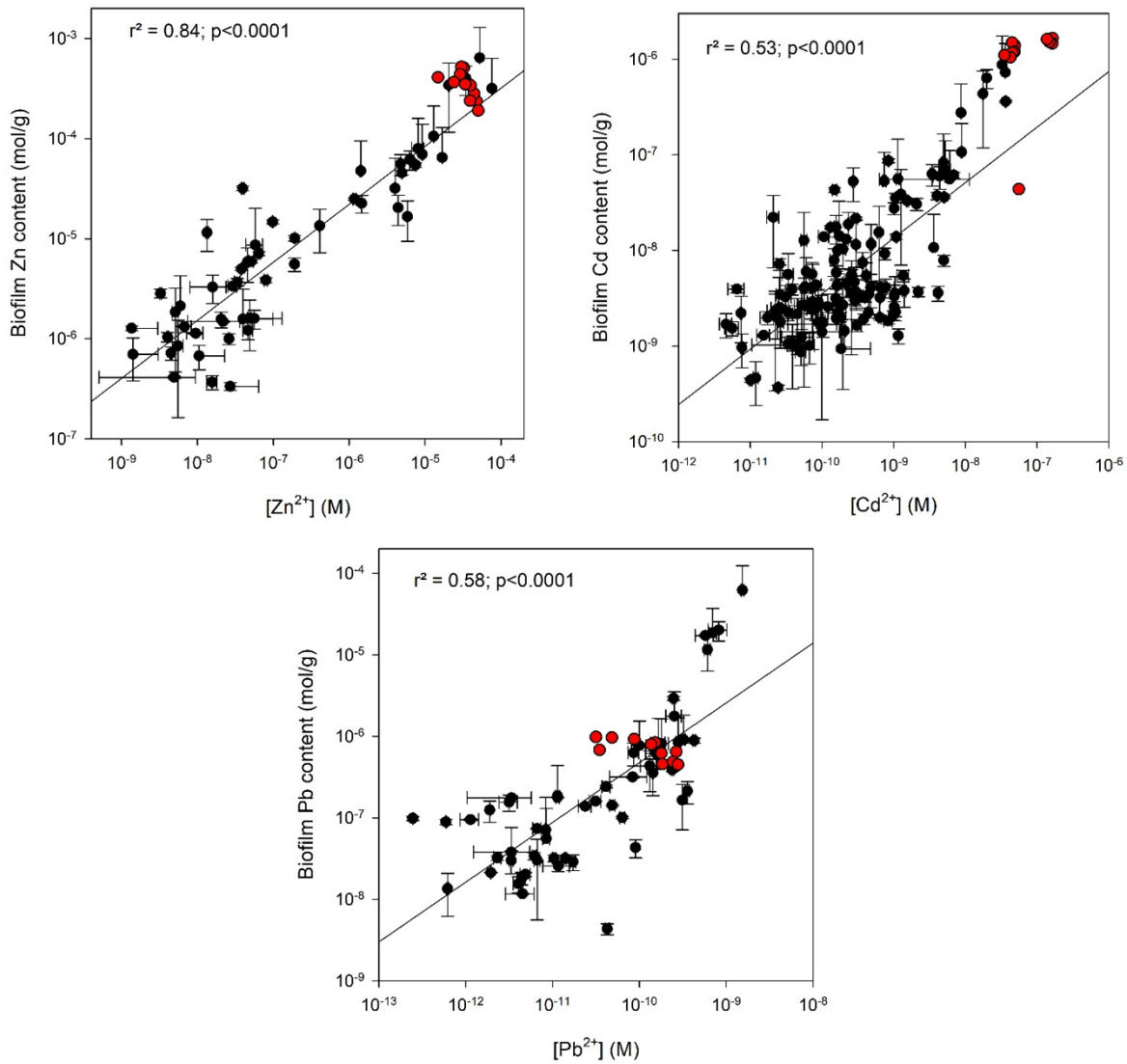

414

415 Figure 4: Linear regressions between biofilm metal content (mol·g^{-1} dry weight) plotted as a function of calculated
416 free metal concentration in water. Red circles are the data of this study while black circles correspond to data from
417 Leguay *et al*. (2016) and Laderriere *et al*. (2021, 2020) for which the pH was above 6.0. Error bars represent
418 standard deviations around the mean (n=3). Free metal concentrations in water and bioaccumulated metal content
419 from the current study are presented in supplementary information (Table 3).

3.4. Diatom assemblage composition and frustule deformities

A total of 19 taxa were observed in the samples collected along LEC. *Achnantidium minutissimum* was present in high abundances at all sites, at proportions ranging from 54.5% at DS1 to 92.9% at US5 (Figure 5). All sites were rather similar in their taxonomic composition and abundances, except for DS1. This site was characterized by a high proportion of *Brachysira neglectissima* (33±26%), which has only been observed at this site, as well as a higher proportion of *Gomphonema parvulum* that reached 6±2% compared to low proportions at other sites (maximum of 1.22±0.76% at DS6). The occurrence of these species may be associated with specific environmental factors including iron concentrations in the water and in the biofilm, as well as conductivity (Table 1, Table 2 and Redundancy analysis RDA in Figure 9 in Supplementary Information).

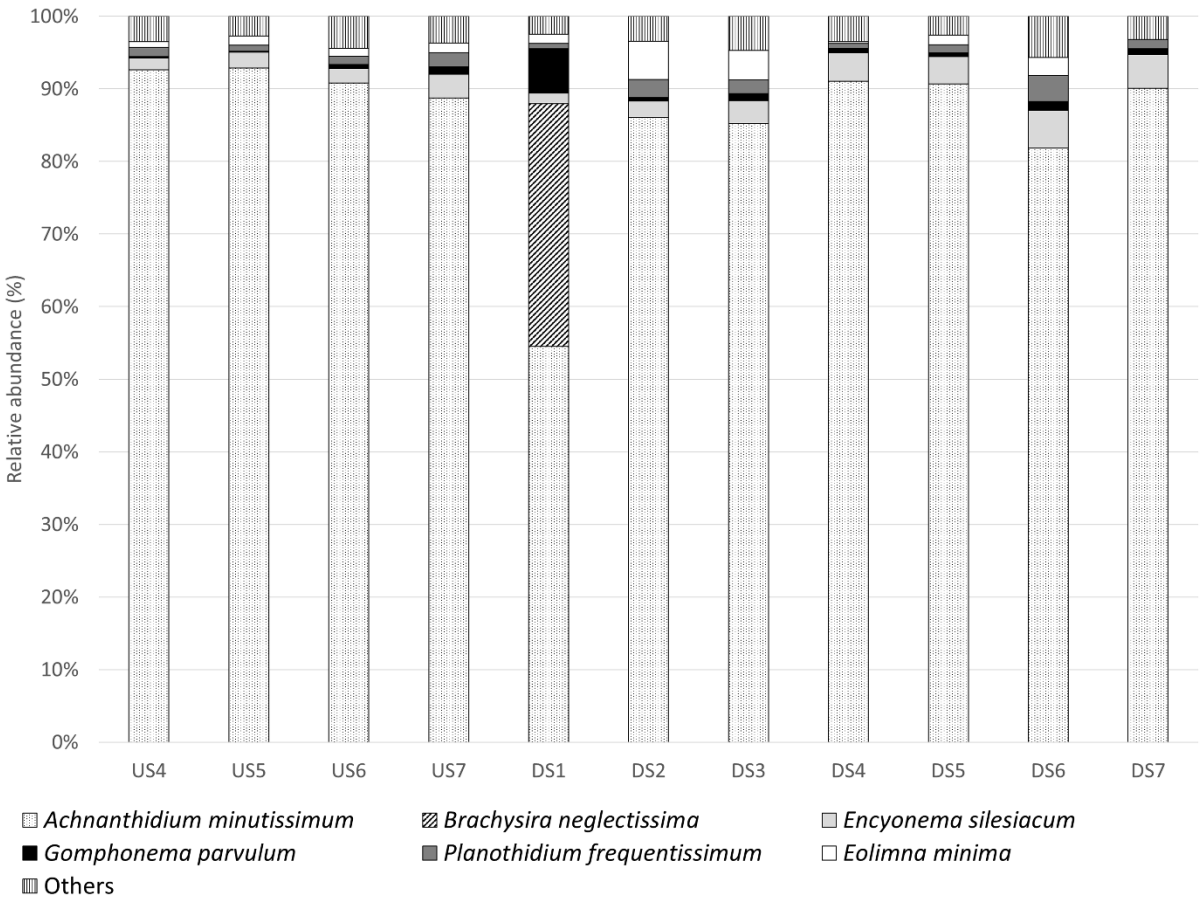

Figure 5: Relative abundance (%) of diatoms species observed in biofilm samples of the Lone Elm Creek. US= Upstream, DS=Downstream (n=4 slides for each site, at least 500 valves were identified on each slide).

The percentage of frustule deformities in periphytic biofilms collected along LEC is presented in Figure 6. Percentage of deformities ranged from 0.9% (US4) to 3% (DS6). Deformities were generally greater than 0.5% in the US and DS reaches, a value considered as the natural threshold of frustule deformities in the absence of contamination (Morin *et al.*, 2008a). In particular, sites US5, US6, DS2, DS3, DS5, DS6, and DS7 have higher occurrence of frustule deformities than 0.5%. However, the teratology occurrence of samples collected upstream and downstream of the mine adit was relatively similar (Student's test, df=42, t=0.58, p-value=0.56), indicating no significant difference of frustule abnormalities between reaches.

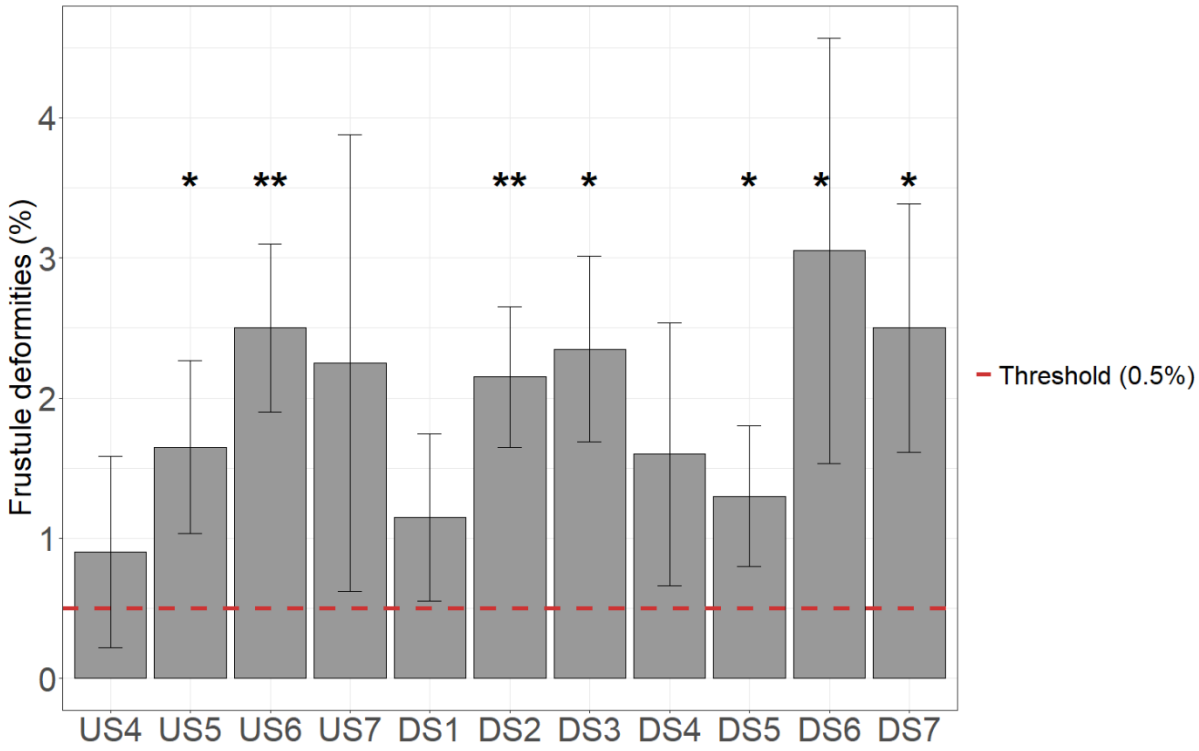

Figure 6: Percentage of total diatom frustules deformities (%) at the sites of Lone Elm Creek. The dashed line represents a threshold value for natural deformities (Morin *et al.*, 2008a) (n=4 slides for each site, at least 500 valves were identified on each slide) (level of significance: *:p-value<0.05, **:p-value<0.01).

Deformities were classified in terms of severity (mild, moderate, severe) and types (overall shape, striation pattern, mixed). Most abnormalities were classified as "mild" (46% in US and 51% in DS) with the exception of sampling site US4 which had a majority of severe deformities (severe=44%, moderate=33% and mild=22%). The other sampling sites with the highest proportions of severe deformities were US6 (28%), US7 (22%), DS2 (23%), DS6 (29%), and DS7 (24%). However, not all species showed deformities or were affected with the

same severity (Supplementary Information, Figure 7). *Achnantidium minutissimum* was the species showing the highest proportions of mild deformities, while *Ulnaria ulna* was generally the species most affected by moderate to severe deformations. *Fragilaria austriaca* also presented high occurrence of deformities (mild, moderate and severe). At DS1, teratological forms of *B. neglectissima* were mostly moderately deformed, whereas *A. minutissimum* was severely deformed. In addition, for both US and DS of the study area, the type of deformation observed seemed to be predominantly affecting the overall shape (over 80%), followed by striae aberrations (15%) and raphe deformations (2%). These deformities were sometimes mixed deformities (15%; affecting the shape as well as the stria or the raphe) (Supplementary Information, Figure 8). In the US reach, mixed deformities accounted for 19% of teratological forms while it accounted for 13% in the DS reach.

4. Discussion

Surprisingly, dissolved metal concentrations were high at our upstream sites, suggesting other metal inputs upstream of the mine adit. Physico-chemical parameters revealed a noteworthy influence of the mine adit, with notable changes in nitrogen, %DO, DOC, and metal concentrations. These physico-chemical changes were accompanied by a change in diatom taxonomic composition at site DS1, but assemblages quickly returned to composition similar to what was observed at all other sites. Diatom deformation results showed relatively homogeneous deformity occurrence, types and severity at all sites, and were observed to be affecting araphid species in particular.

4.1. Water chemistry and dissolved metal concentrations

Water chemistry results revealed a disturbed environment, particularly at DS1, the study site closest to the mine adit. Indeed, DS1 was the site with the highest values for conductivity and NH_4^+ and the lowest values for pH and DOC. This site also exhibited a high concentration of iron in water (Table 2, up to $4x10^{-5}$ mol.L^{-1}) as well as the lowest observed dissolved oxygen value (70%). This abrupt change in %DO is likely related to the unexpected presence of an ammonium peak in parallel with the drastic decrease in NO_3^- following a molar ratio close to 1, as well as the visible precipitation of iron. The peak in ammonium concentrations observed at DS1 suggests a source of organic nitrogen from the mine adit that was degraded into

ammonium. The origin of the mine adit water remains uncertain. It is likely a combination of groundwater, which is often enriched with dissolved organic nitrogen, and stormwater runoff that infiltrates into the shaft through cracks in the surrounding rock.

Under anaerobic conditions, some bacterial strains are able to oxidize Fe(II) by reducing NO_3^- to NH_4^+ (Weber *et al*., 2006). In the absence of oxygen such as in underground water, iron will typically be present in the Fe(II) form. When exposed to oxygen, Fe(II) oxidizes to the less soluble Fe(III) redox form. As shown in Figure 2, iron precipitates were observed at all DS sites. Measured dissolved iron peaked at DS1, suggesting an input of Fe(II) from the mine adit, followed by iron precipitation. In addition, iron precipitates can adsorb and co-precipitate DOC and could also explain the lower DOC value at this site (Chen *et al*., 2014). WHAM calculations also indicated that all measured dissolved iron concentrations were above those expected based on the precipitation of Fe(III) as iron oxyhydroxides.

Metal concentrations did not differ much between upstream and downstream reaches, likely due to historical metal contamination from past land use and mine tailings in the upstream reach and in the area. Located in the downstream portion of the study area, the Eagle Picher smelter has been present since 1881 (Beyer *et al*., 2004) but no longer in operation and could be a legacy source of metal contamination. In addition to soil contamination due to the presence of mine tailings, emissions from the smelter amplifies this contamination in the surrounding terrestrial and aquatic ecosystems (in particular in zinc and lead) through fugitive dust and fallout (Johnson *et al*., 2016). However, the presence of iron precipitates, and in particular iron oxides and hydroxides, may lead to the adsorption of metals such as zinc and cadmium, reducing their concentrations in the water (Biela *et al*., 2019; Dong *et al*., 2007), as observed for cadmium at DS1 (Table 2). CCU values observed in the present study, ranged from 10.4 at DS7 to 35.4 at US5. CCU values were generally higher at upstream sites, which is explained by the higher metal concentrations in the upstream sites compared to downstream sites, in particular for cadmium. Clements *et al*., 2021 investigated benthic macroinvertebrates communities in mining-impacted watersheds in western United States. They showed that CCU values of 2.1 led to a 20% reduction of Ephemeroptera, Plecoptera, and Trichoptera (EPT) richness, while CCU levels exceeding 15.5 led to the elimination of almost 50% of EPT taxa. Thus, high CCU values calculated in the present study may indicate acute and chronic risk of metals to stream communities (for example, macroinvertebrates; Iwasaki *et al*., 2023).

4.2. Metals in biofilms

Biofilm metal contents were different between upstream and downstream sites. While iron concentrations in the water were not significantly different between upstream and downstream sites, iron concentrations in the biofilms collected downstream of the mine adit were higher than in the upstream portion. These biofilms also exhibited a reddish-orange color, in contrast to the biofilms from the sampling points upstream of the discharge area and to the biofilms collected further downstream at DS6 and DS7 which exhibited a green color. As previously mentioned, the reddish-orange color may be an indicator of Fe(III) oxide or hydroxide precipitates formed after oxidation of Fe(II) ions. As the periphyton in the downstream reach was always coated with iron precipitates, it was not possible to collect biofilms without collecting iron oxides and hydroxides at the same time.

4.3. Metal bioaccumulation model

Our data showed a good fit with previous models presented in Laderriere *et al*., (2021, 2020) and Leguay *et al*., (2016), indicating that biofilm accumulated metals (with the focus on zinc, cadmium, and lead) to the same extent as observed elsewhere in North America. As mentioned by Laderriere *et al*., (2020), this relationship suggests that biofilm will internalize a similar quantity of metals for a given free metal concentration in any stream of pH > 6, and that this relationship may be applied to different metal contamination contexts spanning a wide range of geographical areas. It is interesting to note that biofilm cadmium content at the DS1 site is much lower than other data points within the same range of free cadmium concentration, however, this point remains close to the expected value. The low content cadmium in the sbiofilm at this site could be due to cadmium associated with the colloidal fraction. The presence of a colloidal fraction within the mixing zone that would scavenge dissolved cadmium from the water column (Evanko and Dzombak, 1997) could result in lower cadmium accumulation in biofilms and to an overestimated concentration of dissolved Cd (the colloidal fraction would freely cross a 0.45 µm filter membrane).

The balance between metals in water and metals in biofilm is driven by several processes including adsorption to organic and inorganic particles, metal-ligand complex

552 formation, and partitioning between colloidal matter and precipitates (Rose and Shea, 2007).
553 These same processes are influenced by multiple factors including water composition with the
554 presence of major anions and cations, pH, the metal under consideration, and the presence of
555 inorganic or organic ligands. The biofilm matrix offers a large number of sites for metals
556 adsorption such as exopolysaccharides and cell wall of microorganisms (Tien and Chen, 2013).
557 Metals diffuse through the EPS matrix and can be transported within cells by facilitated
558 transport (Bonnineau *et al*., 2020). For example, Ancion *et al*., (2013) suggested that organic
559 matter and fine particle content could increase the metal retention capacity of biofilm and partly
560 explain the enrichment of metals in this complex matrix. Thus, a better characterization of the
561 inorganic and organic content of biofilms could help in explaining certain values that deviate
562 from the model, as in the case of cadmium at site DS1.
563

564 4.4. Diatom assemblages and frustule deformities

565

566 In general, diatom assemblages were homogeneous between upstream and downstream
567 sites, except for DS1. All sites were predominantly composed of *A. minutissimum* which is
568 considered a cosmopolite species found in various environments. The fact that this species
569 dominated the diatom assemblages (75-100%) may also reflect a severe disturbance (Barbour
570 *et al*., 1999). Indeed, *A. minutissimum* is classified as a metal-tolerant species (Cantonati *et al*.,
571 2014; Deniseger *et al*., 1986; Morin *et al*., 2012; Takamura *et al*., 1989). It was reported as a
572 dominant species in zinc- and cadmium-contaminated environments (Ivorra *et al*., 2000) as
573 well as in nickel-contaminated environments (Lavoie *et al*., 2019). Site DS1 showed a marked
574 change in diatom composition, which seems to be partially explained by the iron concentration
575 in the water and in the biofilm and anti-correlated to the concentration of cadmium in the
576 biofilm (See Table 3 and the redundancy analysis RDA in Figure 9 in Supplementary
577 Information). More specifically, a higher proportion of *B. neglectissima* and *G. parvulum* were
578 observed, whereas they were little or not present at the other sites sampled. *G. parvulum* has
579 also been described as a metal tolerant species (Morin *et al*., 2012), associated with disturbed
580 environments, which can adapt to a wide range of physical and chemical stresses. Sabater, 2000
581 observed that *G. parvulum* was almost the only species (along with *Nitzschia palea*) able to
582 withstand metal pollution from a spill that occurred in the Guadiamar River (Spain, in 1999).
583 The species *B. neglectissima* has been described as being able to develop in oligotrophic to
584 dystrophic environments (Leira *et al*., 2017). The high abundance of this species downstream

585 of the mine adit is in accordance with the work of Spitale *et al*., (2011) who observed *B.*
586 *neglectissima* to be more abundant within urbanized areas. In contaminated aquatic
587 ecosystems, tolerant diatom species such as *B. neglectissima* or *G. parvulum* may out-compete
588 sensitive species (Ivorra *et al*., 2002) and thus altering the structure of diatom assemblages
589 (Cattaneo *et al*., 2004). Overall, diatom species richness was low, with only 19 taxa observed
590 throughout the study area. Low diatom richness has also been observed in other metal-
591 contaminated streams studied in Eastern Canada (e.g., Lavoie *et al*., 2012; Leguay *et al*., 2016).
592 While the low richness observed in the cited studies may be attributed to elevated metal
593 concentrations, it can also reflect low nutrients and/or low pH. In the case of LEC, pH values
594 were above 7, but nutrient concentrations were moderate for nitrogen and relatively low for
595 phosphorus, which may partly explain the low diatom richness observed.
596 No clear pattern of deformity occurrence was observed as most of the upstream and
597 downstream sites seemed to present higher average frustules deformities than the natural
598 threshold value estimated at 0.5% (Morin *et al*., 2008a). Interestingly, the closest downstream
599 site to the mine adit, site DS1, showed a low % of deformities. This may be linked to the low
600 dissolved cadmium concentration observed at this site. Pandey *et al*., (2014) showed a strong
601 relationship between intracellular iron and zinc content and the occurrence of diatom frustule
602 deformities. However, it appears that other authors found no relationship between metal
603 concentrations and diatom deformity frequencies (Fernandes da Silva *et al*., 2008; Fernández
604 *et al*., 2018; Lavoie *et al*., 2012; Leguay *et al*., 2016), and that is the case also in the present
605 study.
606 In our study, only certain species were deformed. Long and narrow araphid species such
607 as *U. ulna* and *F. austriaca* were the most frequently deformed and generally presented
608 moderate and severe aberrations of the overall shape. This finding is in accordance with other
609 studies suggesting that rapheless diatoms seem to be more prone to teratologies compared to
610 other species (Silva *et al*., 2009, Lavoie *et al*., 2012, Pandey *et al*., 2018). Few studies reported
611 the proportion of each type of diatom frustule abnormalities. For example, Pandey *et al*., (2014)
612 observed that in conditions of zinc and lead contamination, diatoms had a majority of striae
613 deformities and also often exhibited mixed deformities. In this study, among the different forms
614 of deformities, the most common were those affecting the frustule shape (80%). This shape
615 deformity is probably transmitted to subsequent generations during cell division as the daughter
616 cell needs to form a new valve that fits the deformed valve from the mother cell (Lavoie *et al*.,
617 2017). For this reason, this type of deformity may possibly lead to an overestimation of the

response to contamination compared to other types of deformities that are not transmitted during cell division.

The presence in large proportions of very small taxa such as *A. minutissimum*, which are difficult to observe under an optical microscope, can lead to an underestimation of deformities as certain deformities may be missed (Morin *et al*., 2008b). Additionally, metal contamination can select for certain small, tolerant species (Morin *et al*., 2008a), further contributing to a potential underestimation of metal contamination and to variability in the response of this biomarker. In addition, small species such as *A. minutissimum* often settle in girdle view (side view) which further complicates the observation of potential deformities. It is also sometimes difficult to determine whether the observed deformities are normal phenotypic variations or the consequence of exposure to a contaminant (Cantonati *et al*., 2014).

5. Conclusion

The results from this study showed that the LEC in Joplin, Missouri located within the Tri-State Mining District, is substantially contaminated in iron, zinc, cadmium, and lead. Surprisingly, dissolved metal concentrations were relatively homogeneous along the studied transect, regardless of the mine adit. This finding highlighted the possible effects of multiple sources of metal contamination. Physico-chemical parameters, biofilm metal bioaccumulation and diatom assemblages revealed a strong impact of metallic contamination at the first site downstream of the mine adit. In addition, iron, lead, and zinc were measured in higher concentrations in the sites downstream of the mine adit compared to the sites in the upper portion of the study area. The presence of diatom deformities was a red flag indicating a response of these microalgae to metal contamination, but a clear relationship with metal concentrations was not observed. As previously suggested, the percent occurrence of diatom deformities may not be the most appropriate biomarker to relate the magnitude of a response to stress as a function of metal concentrations. Finally, the data from Lone Elm Creek seemed to fit well with previously published predictive models, underscoring once again the potential universal relationship between free metal ions in the water and their bioaccumulation in the biofilm. This provides evidence for the reliable use of bioaccumulated metals in biofilm as proxies of metal exposure.

References

Wen C, Li Q, Zhu D, Zhong M, Zhu S, Xu H, Li C, Zhu S, Caiola N, Chen L, Luo X (2024) Biofilm-mediated heavy metal bioaccumulation and trophic transfer in a mining-contaminated river.

Fadhlaoui, M., Pearce, N.J.T., Lavoie, I., Fortin, C., 2024. Interactive effects of bismuth exposure (water and diet) and temperature on snail fatty acid composition, antioxidant enzymes and lipid peroxidation. Frontiers in Environmental Chemistry 5, 1332967. https://doi.org/10.3389/fenvc.2024.1332967

Wen, C., Li, Q., Zhu, D., Zhong, M., Zhu, Shijun, Xu, H., Li, C., Zhu, Shiqi, Caiola, N., Chen, L., Luo, X., 2024. Biofilm-mediated heavy metal bioaccumulation and trophic transfer in a mining-contaminated river. Water Research 267, 122487. https://doi.org/10.1016/j.watres.2024.122487

Xie, L., Funk, D.H., Buchwalter, D.B., 2010. Trophic transfer of Cd from natural periphyton to the grazing mayfly Centroptilum triangulifer in a life cycle test. Environmental Pollution 158, 272–277. https://doi.org/10.1016/j.envpol.2009.07.010

Ali, H., Khan, E., 2019. Trophic transfer, bioaccumulation, and biomagnification of non-essential hazardous heavy metals and metalloids in food chains/webs—Concepts and implications for wildlife and human health. Human and Ecological Risk Assessment: An International Journal 25, 1353–1376. https://doi.org/10.1080/10807039.2018.1469398

Ancion, P.-Y., Lear, G., Dopheide, A., Lewis, G.D., 2013. Metal concentrations in stream biofilm and sediments and their potential to explain biofilm microbial community structure. Environmental Pollution 173, 117–124. https://doi.org/10.1016/j.envpol.2012.10.012

Balasubramaniam, K., Rühland, K.M., Smol, J.P., 2023. A diatom-based paleolimnological re-assessment of previously polymictic Lake Opinicon, Ontario (Canada): crossing an ecological threshold in response to warming over the past 25 years. Journal of Paleolimnology 69, 37–55. https://doi.org/10.1007/s10933-022-00261-w

Barbour, M., Gerritsen, J., Snyder, B., Stribling, J.B., 1999. Rapid bioassessment protocols for use in streams and wadeable rivers: Periphyton, benthic macroinvertebrates, and fish, 2nd edition. EPA 841-B-99-002. US Environmental Protection Agency, Office of Water.

Battin, T.J., Besemer, K., Bengtsson, M.M., Romani, A.M., Packmann, A.I., 2016. The ecology and biogeochemistry of stream biofilms. Nature Reviews Microbiology 14, 251–263. https://doi.org/10.1038/nrmicro.2016.15

Bey, M.-Y., Ector, L., 2013. Atlas des diatomees des cours d'eau de la region Rhone-Alpes. Tome 1. Centriques, Monoraphidees. Tome 2. Araphidees, Brachyraphidees. Tome 3. Naviculacees: Naviculoidees. Tome 4. Naviculacees: Naviculoidees. Tome 5. Naviculacees: Cymbelloidees, Gomphonematoidees. Tome 6. Bacillariacees, Rhopalodiacees, Surirellacees. Direction regionale de l'Environnement, de l'Amenagement et du Logement Rhone-Alpes, Lyon.

Beyer, W.N., Dalgarn, J., Dudding, S., French, J.B., Mateo, R., Miesner, J., Sileo, L., Spann, J., 2004. Zinc and Lead Poisoning in Wild Birds in the Tri-State Mining District (Oklahoma, Kansas, and Missouri). Archives of Environmental Contamination and Toxicology 48, 108–117. https://doi.org/10.1007/s00244-004-0010-7

Biela, R., Kucera, T., Konecny, J., 2019. Use of Sorption Materials for Removing Cadmium from Water. IOP Conference Series: Earth and Environmental Science 221, 012133. https://doi.org/10.1088/1755-1315/221/1/012133

Blinn, D.W., Fredericksen, A., Korte, V., 1980. Colonization rates and community structure of diatoms on three different rock substrata in a lotic system. British Phycological Journal 15, 303–310. https://doi.org/10.1080/00071618000650311

Bonada, N., Prat, N., Resh, V.H., Statzner, B., 2006. Developments in aquatic insect biomonitoring: A Comparative Analysis of Recent Approaches. Annual Review of Entomology 51, 495–523. https://doi.org/10.1146/annurev.ento.51.110104.151124

Bonnineau, C., Artigas, J., Chaumet, B., Dabrin, A., Faburé, J., Ferrari, B.J.D., Lebrun, J.D., Margoum, C., Mazzella, N., Miège, C., Morin, S., Uher, E., Babut, M., Pesce, S., 2020. Role of Biofilms in Contaminant Bioaccumulation and Trophic Transfer in Aquatic Ecosystems: Current State of Knowledge and Future Challenges, in: de Voogt, P. (Ed.), Reviews of Environmental Contamination and Toxicology Volume 253, Springer International Publishing, Cham, pp. 115–153. https://doi.org/10.1007/398_2019_39

Bradac, P., Wagner, B., Kistler, D., Traber, J., Behra, R., Sigg, L., 2010. Cadmium speciation and accumulation in periphyton in a small stream with dynamic concentration variations. Environmental Pollution 158, 641–648. https://doi.org/10.1016/j.envpol.2009.10.031

Buss, D.F., Carlisle, D.M., Chon, T.-S., Culp, J., Harding, J.S., Keizer-Vlek, H.E., Robinson, W.A., Strachan, S., Thirion, C., Hughes, R.M., 2015. Stream biomonitoring using macroinvertebrates around the globe: a comparison of large-scale programs. Environmental Monitoring and Assessment 187, 4132. https://doi.org/10.1007/s10661-014-4132-8

Campbell, P.G.C., Errécalde, O., Fortin, C., Hiriart-Baer, V.P., Vigneault, B., 2002. Metal bioavailability to phytoplankton—applicability of the biotic ligand model. Comparative Biochemistry and Physiology Part C: Toxicology & Pharmacology 133, 189–206. https://doi.org/10.1016/S1532-0456(02)00104-7

Cantonati, M., Angeli, N., Virtanen, L., Wojtal, A.Z., Gabrieli, J., Falasco, E., Lavoie, I., Morin, S., Marchetto, A., Fortin, C., Smirnova, S., 2014. Achnanthidium minutissimum (Bacillariophyta) valve deformities as indicators of metal enrichment in diverse widely-distributed freshwater habitats. Science of the Total Environment 475, 201–215. https://doi.org/10.1016/j.scitotenv.2013.10.018

Cattaneo, A., Couillard, Y., Wunsam, S., Courcelles, M., 2004. Diatom taxonomic and morphological changes as indicators of metal pollution and recovery in Lac Dufault (Québec, Canada). Journal of Paleolimnology 32, 163–175. https://doi.org/10.1023/B:JOPL.0000029430.78278.a5

Charles, D.F., Tuccillo, A.P., Belton, T.J., 2019. Use of diatoms for developing nutrient criteria for rivers and streams: A Biological Condition Gradient approach. Ecological Indicators 96, 258–269. https://doi.org/10.1016/j.ecolind.2018.08.048

Chen, C., Dynes, J.J., Wang, J., Sparks, D.L., 2014. Properties of Fe-Organic Matter Associations via Coprecipitation versus Adsorption. Environmental Science & Technology 48, 13751–13759. https://doi.org/10.1021/es503669u

Clements, W.H., Carlisle, D.M., Lazorchak, J.M., Johnson, P.C., 2000. Heavy metals structure benthic communities in Colorado mountain streams. Ecological Applications 10. https://doi.org/10.2307/2641120.

Clements, W.H., Herbst, D.B., Hornberger, M.I., Mebane, C.A., Short, T.M., 2021. Long-term monitoring reveals convergent patterns of recovery from mining contamination

across 4 western US watersheds. Freshwater Science 40, 407–426. https://doi.org/10.1086/714575

Deniseger, J., Austin, A., Lucey, W.P., 1986. Periphyton communities in a pristine mountain stream above and below heavy metal mining operations. Freshwater Biology 16, 209–218. https://doi.org/10.1111/j.1365-2427.1986.tb00965.x

Dong, D., Zhao, X., Hua, X., Zhang, J., Wu, S., 2007. Lead and Cadmium Adsorption onto Iron Oxides and Manganese Oxides in the Natural Surface Coatings Collected on Natural Substances in the Songhua River of China. Chemical Research in Chinese Universities 23, 659–664. https://doi.org/10.1016/S1005-9040(07)60143-3

Evanko, C.R., Dzombak, D.A., 1997. Remediation of metals-contaminated soils and groundwater. Department of Civil and Environmental Engineering, Ground-water remediation technologies analysis center, Carnegie Mellon University, PA.

Fadhlaoui, Mariem, Nolan J. T. Pearce, Isabelle Lavoie, et Claude Fortin. Interactive effects of bismuth exposure (water and diet) and temperature on snail fatty acid composition, antioxidant enzymes and lipid peroxidation . Frontiers in Environmental Chemistry. 5-2024. https://doi.org/10.3389/fenvc.2024.1332967.

Falasco, E., Ector, L., Wetzel, C.E., Badino, G., Bona, F., 2021. Looking back, looking forward: a review of the new literature on diatom teratological forms (2010–2020). Hydrobiologia 848, 1675–1753. https://doi.org/10.1007/s10750-021-04540-x

Fernandes da Silva, C., Ballester, E., Monserrat, J., Geracitano, L., Wasielesky Jr, W., Abreu, P.C., 2008. Contribution of microorganisms to the biofilm nutritional quality: protein and lipid contents. Aquaculture Nutrition 14, 507–514. https://doi.org/10.1111/j.1365-2095.2007.00556.x

Fernández, M.R., Martín, G., Corzo, J., De La Linde, A., García, E., López, M., Sousa, M., 2018. Design and testing of a new diatom-based index for heavy metal pollution. Archives of Environmental Contamination and Toxicology 74, 170–192. https://doi.org/10.1007/s00244-017-0409-6

Gibson, A.M., 1972. Wilderness Bonanza- the Tri-state District of Missouri, Kansas, and Oklahoma. University of Oklahoma Press, Norman Oklahoma.

Griffith, M.B., Hill, B.H., McCormick, F.H., Kaufmann, P.R., Herlihy, A.T., Selle, A.R., 2005. Comparative application of indices of biotic integrity based on periphyton, macroinvertebrates, and fish to southern Rocky Mountain streams. Ecological Indicators 5, 117–136. https://doi.org/10.1016/j.ecolind.2004.11.001

Guasch, H., Artigas, J., Bonet, B., Bonnineau, C., Canals, O., Corcoll, N., Foulquier, A., Lopez-Doval, J., Kim Tiam, S., Morin, S., Navarro, E., Pesce, S., Proia, L., Salvadó, H., Serra, A., 2016. The use of biofilms to assess the effects of chemicals on freshwater ecosystems. Caister Academic Press pp. 125–144. https://doi.org/10.21775/9781910190173.07

Gutierrez, M., Collette, Z., Mcclanahan, A., Mickus, K., 2019. Mobility of Metals in Sediments Contaminated with Historical Mining Wastes: Example from the Tri-State Mining District, USA. Soil Systems 3. https://doi.org/10.3390/soilsystems3010022

Gutierrez, M., Wu, S.-S., Peebles, J., 2015. Geochemical mapping of Pb- and Zn-contaminated streambed sediments in southwest Missouri, USA. Journal of Soils and Sediments 15. https://doi.org/10.1007/s11368-014-1010-5

Ivorra, N., Barranguet, C., Jonker, M., Kraak, M.H.S., Admiraal, W., 2002. Metal-induced tolerance in the freshwater microbenthic diatom Gomphonema parvulum. Environmental Pollution 116, 147–157. https://doi.org/10.1016/S0269-7491(01)00152-X

Ivorra, N., Bremer, S., Guasch, H., Kraak, M.H.S., Admiraal, W., 2000. Differences in the sensitivity of benthic microalgae to ZN and CD regarding biofilm development and exposure history. Environmental Toxicology and Chemistry 19, 1332–1339. https://doi.org/10.1002/etc.5620190516

Iwasaki, Y., Mano, H., Shinohara, N., 2023. Linking levels of trace-metal concentrations and ambient toxicity to cladocerans to levels of effects on macroinvertebrate communities. Environmental Advances 11, 100348. https://doi.org/10.1016/j.envadv.2023.100348

Johnson, A.W., Gutiérrez, M., Gouzie, D., McAliley, L.R., 2016. State of remediation and metal toxicity in the Tri-State Mining District, USA. Chemosphere 144, 1132–1141. https://doi.org/10.1016/j.chemosphere.2015.09.080

Laderriere, V., Le Faucheur, S., Fortin, C., 2021. Exploring the role of water chemistry on metal accumulation in biofilms from streams in mining areas. Science of the Total Environment 784, 146986. https://doi.org/10.1016/j.scitotenv.2021.146986

Laderriere, V., Paris, L.-E., Fortin, C., 2020. Proton Competition and Free Ion Activities Drive Cadmium, Copper, and Nickel Accumulation in River Biofilms in a Nordic Ecosystem. Environments 7, 112. https://doi.org/10.3390/environments7120112

Laderriere, V., Richard, M., Morin, S., Le Faucheur, S., Fortin, C., 2022. Temperature and Photoperiod Affect the Sensitivity of Biofilms to Nickel and its Accumulation. Environmental Toxicology and Chemistry 41, 1649–1662. https://doi.org/10.1002/etc.5335

Lavoie, I., Campeau, S., Zugic-Drakulic, N., Winter, J.G., Fortin, C., 2014. Using diatoms to monitor stream biological integrity in Eastern Canada: An overview of 10 years of index development and ongoing challenges. Science of the Total Environment 475, 187–200. https://doi.org/10.1016/j.scitotenv.2013.04.092

Lavoie, I., Grenier, M., Campeau, S., Dillon, P.J., 2010. The Eastern Canadian Diatom Index (IDEC) Version 2.0: Including Meaningful Ecological Classes and an Expanded Coverage Area that Encompasses Additional Geological Characteristics. Water Quality Research Journal 45, 463–477. https://doi.org/10.2166/wqrj.2010.045

Lavoie, I., Hamilton, P.B., Campeau, S., Grenier, M., Dillon, P.J., 2008. Guide d'identification des diatomées des rivières de l'Est du Canada, 1st ed. Presses de l'Université du Québec. https://doi.org/10.2307/j.ctv18ph4tz

Lavoie, I., Hamilton, P.B., Morin, S., Kim Tiam, S., Kahlert, M., Gonçalves, S., Falasco, E., Fortin, C., Gontero, B., Heudre, D., Kojadinovic-Sirinelli, M., Manoylov, K., Pandey, L.K., Taylor, J.C., 2017. Diatom teratologies as biomarkers of contamination: Are all deformities ecologically meaningful? Ecological Indicators 82, 539–550. https://doi.org/10.1016/j.ecolind.2017.06.048

Lavoie, I., Lavoie, M., Fortin, C., 2012. A mine of information: Benthic algal communities as biomonitors of metal contamination from abandoned tailings. Science of the Total Environment 425, 231–241. https://doi.org/10.1016/j.scitotenv.2012.02.057

Lavoie, I., Morin, S., Laderriere, V., Fortin, C., 2018. Freshwater Diatoms as Indicators of Combined Long-Term Mining and Urban Stressors in Junction Creek (Ontario, Canada). Environments 5, 30. https://doi.org/10.3390/environments5020030

Lavoie, I., Morin, S., Laderriere, V., Paris, L.-E., Fortin, C., 2019. Assessment of Diatom Assemblages in Close Proximity to Mining Activities in Nunavik, Northern Quebec (Canada). Environments 6, 74. https://doi.org/10.3390/environments6060074

Lavoie, M., Campbell, P.G.C., Fortin, C., 2016. Importance de mieux connaître les mécanismes de transport des métaux pour la prédiction de l'accumulation et de la toxicité des métaux dissous chez le phytoplancton : récentes avancées et défis pour le développement du modèle du ligand biotique. rseau 29, 119–147. https://doi.org/10.7202/1036544ar

Leguay, S., Lavoie, I., Levy, J.L., Fortin, C., 2016. Using biofilms for monitoring metal contamination in lotic ecosystems: The protective effects of hardness and pH on metal bioaccumulation: Monitoring metal contamination using stream biofilms. Environmental Toxicology and Chemistry 35, 1489–1501. https://doi.org/10.1002/etc.3292

Lei, Y., Wang, Y., Qin, F., Liu, J., Feng, P., Luo, L., Jordan, R.W., Jiang, S., 2021. Diatom assemblage shift driven by nutrient dynamics in a large, subtropical reservoir in southern China. Journal of Cleaner Production 317, 128435. https://doi.org/10.1016/j.jclepro.2021.128435

Leira, M., López-Rodríguez, M.D.C., Carballeira, R., 2017. Epilithic diatoms (Bacillariophyceae) from running watersin NW Iberian Peninsula (Galicia, Spain). Anales del Jardín Botánico de Madrid 74, 062. https://doi.org/10.3989/ajbm.2421

Lobo, E.A., Heinrich, C.G., Schuch, M., Wetzel, C.E., Ector, L., 2016. Diatoms as Bioindicators in Rivers, in: Necchi JR, O. (Ed.), River Algae. Springer International Publishing, Cham, pp. 245–271. https://doi.org/10.1007/978-3-319-31984-1_11

McCauley, J.R, Brady, L.L, Wilson, F.W, 1983. A Study of Stability Problems and Hazard Evaluation of the Kansas Portion of the Tri-state Mining Area: Kansas Geological Survey.

Morin, Duong, Dabrin, Coynel, Herlory, O., Baudrimont, M., Delmas, F., Durrieu, G., Schäfer, J., Winterton, P., Blanc, G., Coste, M., 2008. Long-term survey of heavy-metal pollution, biofilm contamination and diatom community structure in the Riou Mort watershed, South-West France. Environmental Pollution 151, 532–542. https://doi.org/10.1016/j.envpol.2007.04.023

Morin, S., Cordonier, A., Lavoie, I., Arini, A., Blanco, S., Duong, T.T., Tornés, E., Bonet, B., Corcoll, N., Faggiano, L., Laviale, M., Pérès, F., Becares, E., Coste, M., Feurtet-Mazel, A., Fortin, C., Guasch, H., Sabater, S., 2012. Consistency in Diatom Response to Metal-Contaminated Environments, in: Guasch, H., Ginebreda, A., Geiszinger, A. (Eds.), Emerging and Priority Pollutants in Rivers, The Handbook of Environmental Chemistry. Springer Berlin Heidelberg, Berlin, Heidelberg, pp. 117–146. https://doi.org/10.1007/978-3-642-25722-3_5

Morin, S., Coste, M., Hamilton, P.B., 2008. Scanning electron microscopy observations of deformities in small pennate diatoms exposed to high cadmium concentrations. Journal of Phycology 44, 1512–1518.

National oceanic and atmospheric administration, 2020. National Weather Service [WWW Document]. URL https://www.weather.gov/

Nziguheba, G., Smolders, E., 2008. Inputs of trace elements in agricultural soils via phosphate fertilizers in European countries. Science of the Total Environment 390, 53–57. https://doi.org/10.1016/j.scitotenv.2007.09.031

Pandey, L.K., Kumar, D., Yadav, A., Rai, J., Gaur, J.P., 2014. Morphological abnormalities in periphytic diatoms as a tool for biomonitoring of heavy metal pollution in a river. Ecological Indicators 36, 272–279. https://doi.org/10.1016/j.ecolind.2013.08.002

Pandey, L.K., Lavoie, I., Morin, S., Park, J., Lyu, J., Choi, S., Lee, H., Han, T., 2018. River water quality assessment based on a multi-descriptor approach including chemistry, diatom assemblage structure, and non-taxonomical diatom metrics. Ecological Indicators 84, 140–151. https://doi.org/10.1016/j.ecolind.2017.07.043

Pillsbury, R.W., Reavie, E.D., Estepp, L.R., 2021. Diatom and geochemical paleolimnology reveals a history of multiple stressors and recovery on Lake Ontario. Journal of Great Lakes Research 47, 1316–1326. https://doi.org/10.1016/j.jglr.2021.07.006

Plessl, C., Otachi, E.O., Körner, W., Avenant-Oldewage, A., Jirsa, F., 2017. Fish as bioindicators for trace element pollution from two contrasting lakes in the Eastern Rift

Valley, Kenya: spatial and temporal aspects. Environmental Science and Pollution Research 24, 19767–19776. https://doi.org/10.1007/s11356-017-9518-z
Prygiel, J., Carpentier, P., Almeida, S., Coste, M., Druart, J.-C., Ector, L., Guillard, D., Honoré, M.-A., Iserentant, R., Ledeganck, P., Lalanne-Cassou, C., Lesniak, C., Mercier, I., Moncaut, P., Nazart, M., Nouchet, N., Peres, F., Peeters, V., Rimet, F., Rumeau, A., Sabater, S., Straub, F., Torrisi, M., Tudesque, L., Van De Vijver, B., Vidal, H., Vizinet, J., Zydek, N., 2002. Determination of the biological diatom index (IBD NF T 90–354): results of an intercomparison exercise. Journal of Applied Phycology 14, 27–39. https://doi.org/10.1023/A:1015277207328
Rimet, F., 2012. Recent views on river pollution and diatoms. Hydrobiologia 683, 1–24. https://doi.org/10.1007/s10750-011-0949-0
Rimet, F., Bouchez, A., 2011. Use of diatom life-forms and ecological guilds to assess pesticide contamination in rivers: Lotic mesocosm approaches. Ecological Indicators 11, 489–499. https://doi.org/10.1016/j.ecolind.2010.07.004
Rose, S., Shea, J.A., 2007. Chapter 6 Environmental geochemistry of trace metal pollution in urban watersheds, in: Developments in Environmental Science. Elsevier, pp. 99–131. https://doi.org/10.1016/S1474-8177(07)05006-1
Sabater, S., 2000. Diatom communities as indicators of environmental stress in the Guadiamar River, S-W. Spain, following a major mine tailings spill. Journal of Applied Phycology 12, 113–124. https://doi.org/10.1023/A:1008197411815
Sabater, S., Guasch, H., Ricart, M., Romaní, A., Vidal, G., Klünder, C., Schmitt-Jansen, M., 2007. Monitoring the effect of chemicals on biological communities. The biofilm as an interface. Analytical and Bioanalytical Chemistry 387, 1425–1434. https://doi.org/10.1007/s00216-006-1051-8
Smucker, N.J., Vis, M.L., 2009. Use of diatoms to assess agricultural and coal mining impacts on streams and a multiassemblage case study. Journal of the North American Benthological Society 28, 659–675. https://doi.org/10.1899/08-088.1
Spitale, D., Scalfi, A., Lange-Berthalot, H., Cantonati, M., 2011. Using different epilithic-diatom assemblage metrics for an ecological characterization of the shores of Lake Garda. Journal of Limnology 70, 197–208. https://doi.org/10.3274/jl11-70-2-11
Stefanowicz, A.M., Woch, M.W., Kapusta, P., 2014. Inconspicuous waste heaps left by historical Zn–Pb mining are hot spots of soil contamination. Geoderma 235–236, 1–8. https://doi.org/10.1016/j.geoderma.2014.06.020
Takamura, N., Kasai, F., Watanabe, M.M., 1989. Effects of Cu, Cd and Zn on photosynthesis of freshwater benthic algae. Journal of Applied Phycology 1, 39–52. https://doi.org/10.1007/BF00003534
Thompson, T.L., 1995. The Stratigraphic Succession In Missouri (Revised 1995). Missouri Department of Natural Resources, Division of Geology and Land Survey.
Tien, C.-J., Chen, C.S., 2013. Patterns of Metal Accumulation by Natural River Biofilms During Their Growth and Seasonal Succession. Archives of Environmental Contamination and Toxicology 64, 605–616. https://doi.org/10.1007/s00244-012-9856-2
Tipping, E., Lofts, S., Sonke, J.E., 2011. Humic Ion-Binding Model VII: a revised parameterisation of cation-binding by humic substances. Environmental Chemistry 8, 225. https://doi.org/10.1071/EN11016
U.S. Geological Survey, 2019. Water Quality Samples for Missouri: Sample Data [WWW Document]. URL https://tinyurl.com/msn8vw5b
USEPA, 2023. National Recommended Water Quality Criteria - Aquatic Life Criteria Table [WWW Document]. URL https://www.epa.gov/wqc/national-recommended-water-quality-criteria-aquatic-life-criteria-table

USEPA, 2020. Oronogo-duenweg mining belt, Joplin, MO, Cleanup Activities. United States Environmental Protection Agency. URL https://tinyurl.com/2p8a5r9x

Virta, L., Teittinen, A., 2022. Threshold effects of climate change on benthic diatom communities: Evaluating impacts of salinity and wind disturbance on functional traits and benthic biomass. Science of the Total Environment 826, 154130. https://doi.org/10.1016/j.scitotenv.2022.154130

Weber, K.A., Urrutia, M.M., Churchill, P.F., Kukkadapu, R.K., Roden, E.E., 2006. Anaerobic redox cycling of iron by freshwater sediment microorganisms. Environmental Microbiology 8, 100–113. https://doi.org/10.1111/j.1462-2920.2005.00873.x

Wen, H., Zhu, C., Zhang, Y., Cloquet, C., Fan, H., Fu, S., 2016. Zn/Cd ratios and cadmium isotope evidence for the classification of lead-zinc deposits. Scientific Reports 6, 25273. https://doi.org/10.1038/srep25273

Wetzel, R.G. (Ed.), 1983. Periphyton of Freshwater Ecosystems: Proceedings of the First International Workshop on Periphyton of Freshwater Ecosystems held in Växjö, Sweden, 14–17 September 1982. Springer Netherlands, Dordrecht. https://doi.org/10.1007/978-94-009-7293-3

Wilson, J., 2023. Impacts of legacy mining on stream structural and functional processes in an urban stream. PhD Thesis. University of Missouri-Columbia, Natural Resources (MU), USA 320 pp.

Zhang, Y., Lu, X., Wang, N., Xin, M., Geng, S., Jia, J., Meng, Q., 2016. Heavy metals in aquatic organisms of different trophic levels and their potential human health risk in Bohai Bay, China. Environmental Science and Pollution Research 23, 17801–17810. https://doi.org/10.1007/s11356-016-6948-y

Zhao, C.-M., Campbell, P.G.C., Wilkinson, K.J., 2016. When are metal complexes bioavailable? Environmental Chemistry 13, 425. https://doi.org/10.1071/EN15205